LIQUID CRYSTALS, VOL. 31, NO. 3, MARCH 2004, 377–385

Taylor & Francis
Taylor & Francis Group

Field-induced reorientation dynamics of a surface stabilized ferroelectric liquid crystal mixture

WEN-TSE SHIH, JUNG Y. HUANG*
Institute of Electro-optical Engineering, National Chiao Tung University, Hsinchu, Taiwan ROC

and JING Y. ZHANG
Department of Physics, Georgia Southern University, Statesboro, Georgia, USA

(*Received 2 May 2003; in final form 10 November 2003; accepted 18 November 2003*)

Time-resolved measurements of electro-optical response and Fourier-transform infrared absorption have been employed to study the submolecular motion of a surface stabilized ferroelectric liquid crystal (SSFLC) mixture during a field-induced reorientation process. All observed submolecular groups were found to rotate in unison about the layer normal in a steady d.c. field. In a transient situation, the FLC director can respond rapidly to a pulsed driving field. However, the orientation distribution was found to spread at first and then slowly converge to the new direction of the FLC director. When the field is switched off, all the core groups relax to a steady-state direction with varying relaxation times. The results reveal that submolecular fragments of different molecular species in the FLC mixture move correlatively in a steady d.c. field and during a field-induced reorientation process.

1. Introduction

Flat panel displays with ferroelectric liquid crystals (FLCs) exhibit the advantages of fast response, bi-stability and wide viewing angle [1, 2]. The memory-like behaviour of FLC materials also opens up new possibilities in their applications.

The design of new FLC materials often proves frustrating since it is necessary to obtain a material with both a chiral structure and a smectic C* (SmC*) phase. Although the former is often achievable by synthesis, the latter has seemed more a matter of luck. For practical applications a wide thermodynamically stable SmC* phase is generally required. A method for broadening the temperature range of thermodynamically stable SmC* phases is to obtain a eutectic by mixing several LC components. The design of new FLC components is therefore simplified to the doping of chiral compounds into a mixture with a wide thermodynamically stable SmC phase [3]. This approach gains significance in view of the fact that all commercial FLC materials are mixtures. The properties imparted to a mixture by the addition of a chiral component are more relevant to applications than are its properties as the neat liquid.

For the interests of both fundamental research and industrial applications, many efforts have been made to investigate the switching behavior of FLC materials [4–6]. It is important to note that upon the reversal of the sign of an applied field, all the molecules in the ferroelectric phase switch by rotation about a tilt cone. This is basically because coupling with the applied field is through ferroelectric spontaneous polarization, not through coupling with any individual molecular dipoles. An understanding of the switching dynamics of FLC mixtures is therefore useful, not only for the development of novel flat panel displays, but also for the design of new FLC materials.

During the past decade, time-resolved Fourier-transform infrared absorption (trFTIR) spectroscopy has been shown to be a powerful tool for the investigation of orientation and conformation in complex molecular systems [7–10]. In this study, we report that interesting results on the switching dynamics of a surface stabilized FLC (SSFLC) mixture can also be obtained by combining trFTIR with second harmonic generation and time-resolved electro-optical (EO) measurements.

2. Experimental

The SSFLC cells used consist of two CaF_2 plates coated with indium tin oxide (ITO) conducting films and polyimide alignment layers rubbed unidirectionally.

*Author for correspondence; e-mail: jyhuang@cc.nctu.edu.tw

Liquid Crystals ISSN 0267-8292 print/ISSN 1366-5855 online © 2004 Taylor & Francis Ltd
http://www.tandf.co.uk/journals
DOI: 10.1080/02678290310001658363

The substrates were assembled in a homogeneous geometry with 2 μm cell thickness to form a surface stabilized structure. The cell thickness is close to the half-wave thickness of $d_{\lambda/2}=\lambda/(2\Delta n)=1.9\,\mu m$, with $\Delta n=0.17$ and $\lambda=0.633\,\mu m$.

A chevron-mode ferroelectric liquid crystal mixture FELIX 017/100 from Clariant was filled into a test cell at a temperature above the isotropic phase of the FLC mixture. This material is a mixture of homologues, with a fairly wide SmC* range from 73 to $-28^{\circ}C$, and is fairly promising for flat panel display applications. The test cells were slowly cooled to 35°C and then inserted between a pair of crossed polarizers. All our SSFLC cells appear single domain under conoscopic examination.

For probing the electro-optical properties of the SSFLC cells, bipolar square-wave voltage pulses were applied and the optical transmission was measured as a function of time and rotation angle of the test cell about the optical beam propagation direction. A helium-neon laser with a wavelength of 6328 Å was used.

FTIR spectra from 900 to 3500 cm^{-1} with 8 cm^{-1} resolution were recorded with an Oriel MIR-8000 FTIR spectrometer equipped with a liquid nitrogen cooled HgCdTe detector. A bipolar square-wave pulse, similar to that in the EO measurements, was applied to excite the SSFLC cells during the trFTIR measurement [11].

3. Second harmonic generation and polarized Fourier-transform infrared absorption spectroscopy of a surface stabilized ferroelectric liquid crystal

The azimuthal absorption pattern of an infrared beam propagating through a sample can be expressed as [12]

$$A(\Phi)=\frac{N\pi}{3c}\int\left[\mu_g^{(K)}\cdot\hat{E}_{IR}\right]^2 f(\Omega)\mathrm{d}\Omega \tag{1}$$

where N denotes the number density of the Kth IR dipole moment $\mu_g^{(K)}=\partial\mu_g/\partial Q_K$, Φ is the angle between the incident infrared polarization E_{IR} and the laboratory X-axis, and $f(\Omega)$ represents the orientation distribution of $\mu_g^{(K)}$. For normal incidence on the XY-plane (see figure 1), the integrated absorbance by an atomic group with IR dipole moment parallel to the molecular long axis ($\beta=0$) can be expressed as

$$A(\Phi)=(\cos\theta\cos\Phi+\cos\phi\sin\theta\sin\Phi)^2 \tag{2}$$

where θ denotes the cone angle of FL C, and ϕ the azimuthal angle of the molecular long axis relative to the layer normal X_1. The chevron angle δ of the SSFLC is small and can be neglected in this discussion without causing significant difference.

For an atomic group with IR dipole moment perpendicular to the molecular long axis, we can derive a similar equation for the azimuthal pattern of integrated IR absorbance

$$A(\Phi)=\begin{cases}\frac{1}{2}\sin^2(\Phi\mp\theta),\ \phi=\begin{cases}0\\ \pi\end{cases}\\ \frac{1}{8}\left[3-\cos(2\theta)-2\cos^2\theta\cos(2\Phi)\right],\ \phi=\frac{\pi}{2}.\end{cases} \tag{3}$$

Figure 2 presents the calculated IR absorbance patterns for parallel and perpendicular infrared dipole moments. Within the calculation we assume the IR dipoles to be collectively rotated along the layer normal from $\phi=0$ to π by the changing polarity of the applied field. Note that the angular shift of the azimuthal patterns is about twice the apparent cone angle.

The SSFLC structure shown in figure 1 exhibits a C_2

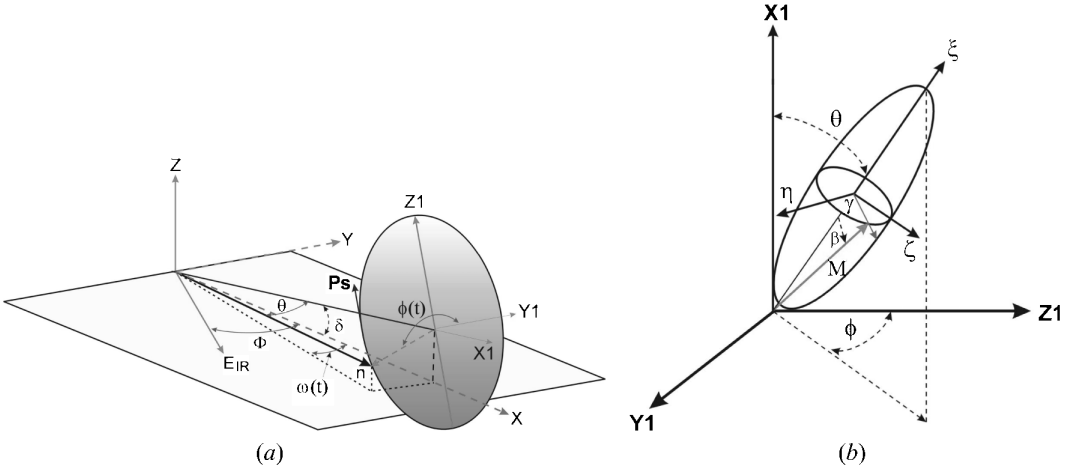

Figure 1. Schematic diagram showing the relationship among the molecular frame ($\xi\eta\zeta$), layer frame ($X_1Y_1Z_1$) and laboratory coordinates system (XYZ).

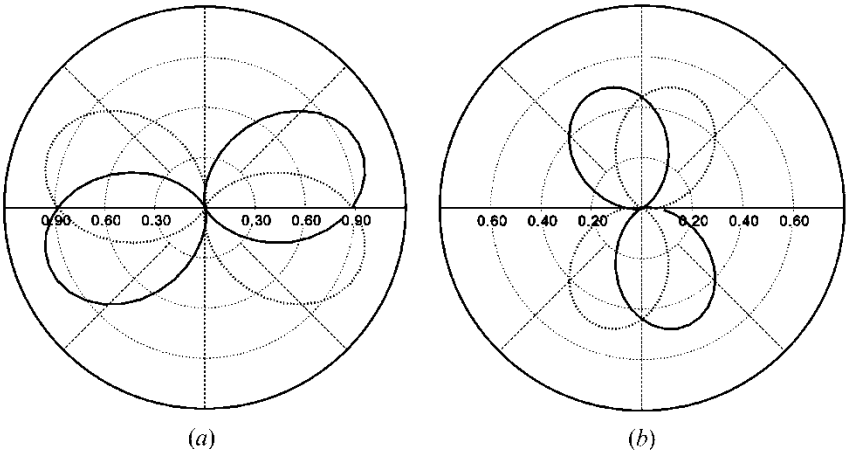

Figure 2. Theoretical curves of the azimuthal FTIR patterns with (*a*) IR dipole moment pointing to $\beta=0^\circ$ or (*b*) $\beta=90^\circ$ of an SSFLC. Here ϕ of the dipole moment is assumed to be 0° (dashed curve) or 180° (solid).

symmetry with the C_2–axis along the Z-axis. The non-vanishing second-order non-linear optical susceptibility components are: $\chi^{(2)}_{ZZZ}$, $\chi^{(2)}_{XXZ}=\chi^{(2)}_{XZX}=\chi^{(2)}_{ZXX}$, $\chi^{(2)}_{YYZ}=\chi^{(2)}_{YZY}=\chi^{(2)}_{ZYY}$, $\chi^{(2)}_{XYZ}=\chi^{(2)}_{YXZ}$, $\chi^{(2)}_{XZY}=\chi^{(2)}_{ZXY}$, $\chi^{(2)}_{YZX}=\chi^{(2)}_{ZYX}$. We calculate the optical second harmonic signal with [13]

$$I_{2\omega}=I^2_{\omega}|\hat{e}_{2\omega}\cdot\chi^{(2)}:\hat{e}_{\omega}\hat{e}_{\omega}|^2. \quad (4)$$

For a rod-shaped FLC molecule we assume that there is a single dominant non-linear polarizability component along the molecular long axis. From equation (4), we note that the chevron FLC structure cannot generate a non-zero SHG signal at normal incidence [14]. SH azimuthal patterns with various optical polarization combinations were therefore calculated by using geometry with an inclined incidence, with the X-axis being along the cell rubbing direction. The results with an SSFLC at $\phi=\pi/2$ are presented in figure 3. No s-polarized SH output can be generated when the cell is excited with an s-polarized fundamental beam. SHG activity also disappears in an SSFLC at $\phi=0^\circ$ or 180°.

4. Results and discussion

4.1. *Steady state properties of an SSFLC*

An SSFLC cell was prepared and characterized by infrared absorption spectroscopy; the results are shown in figure 4. We should emphasize that these IR absorption peaks are composed of contributions from multiple molecular species of the FLC mixture. The observed simplicity of each IR absorption line profile indicates that these molecular species possess high structural similarity. If IR dipoles from different FLC species are not aligned, the resulting azimuthal pattern for each IR absorption line should reveal no clear azimuthal anisotropy. This is also true in a field-induced reorientation process. A clear time-resolved FTIR azimuthal anisotropy indicates a correlated movement of IR dipoles among different FLC species. Therefore an FTIR study on an FLC mixture should yield useful information about the inter-species alignment and field-induced reorientation dynamics which is not available from a study with neat FLC.

Our objective in this study is to determine whether the submolecular fragments of different FLC species in

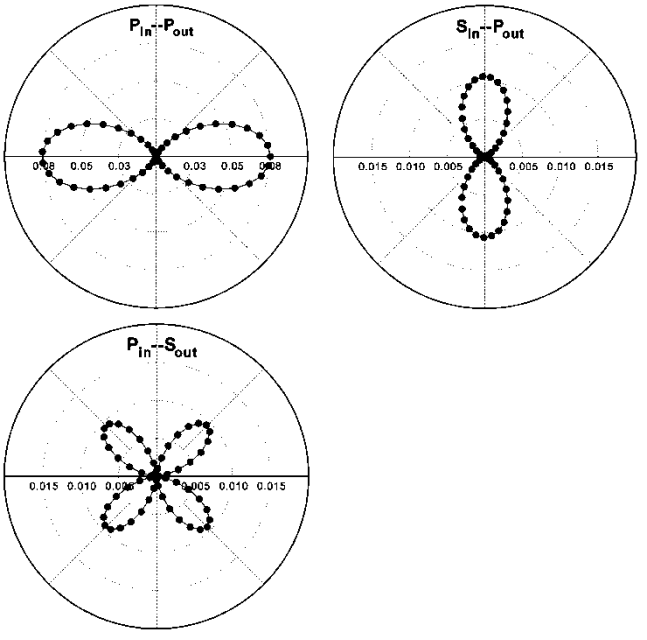

Figure 3. Theoretical curves of azimuthal patterns of second harmonic generation for an SSFLC cell with various optical beam polarization combinations.

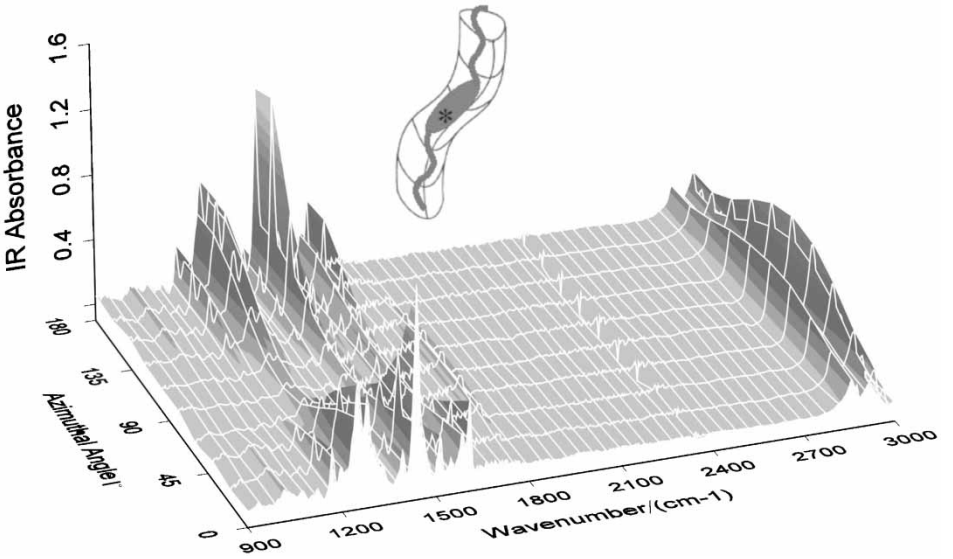

Figure 4. FTIR spectra of an SSFLC measured without applied electric field, plotted as a function of the angle between the incident IR polarization and the rubbing direction of the cell (i.e. the *X*-axis).

an FLC mixture move correlatively in a steady d.c. field or during a field-induced reorientation process. For this purpose, we categorize the observed FTIR absorption lines into two groups: the FLC core modes and modes associated with flexible alkyl chains. The detailed directions of IR dipoles in the molecular frame are therefore somewhat irrelevant. To help further discussion, an effective medium picture with a schematic molecular structure is presented in the inset of figure 4. The schematic structure is distinguished with a rigid core part and flexible alkyl chains. We found that the major features of the IR spectra shown in figure 4 can indeed originate from normal modes associated with the FLC cores at 1169, 1250, 1439, 1516, 1608 and 1763 cm^{-1}; and from the alkyl chains at 2851 and 2924 cm^{-1} [15]. The highest two peaks at 2851 and 2924 cm^{-1} are ascribed to the symmetric and antisymmetric CH_2 stretching along the alkyl chains of the FLC molecules. The peak at 1763 cm^{-1} can be attributed to C=O stretching, and the features at 1608 and 1516 cm^{-1} are mainly from the C=C stretching of the FLC core. The 1439 cm^{-1} peak arises from the combination of the C–C stretch and the in-plane wag of the C–H on the LC core. The remaining normal modes at 1169 and 1250 cm^{-1} are associated with the C–O–C motion.

In figure 4, the rubbing direction of the SSFLC cell is aligned with $\Phi = 0$. The measured azimuthal patterns show that the IR polarizations, which cause maximum absorption by functional groups associated with the FLC core, are all parallel to the averaged molecular long axis. However, for C=O and CH_2 groups the maximum IR absorption occurs with the IR polarization being perpendicular to the averaged molecular long axis. A similar result has also been observed on neat FLC materials [16]. These azimuthal patterns carry information about the averaged direction of IR dipoles. The mutual perpendicularity between the azimuthal patterns of IR absorption lines from the core and alkyl chains can be explained with a zigzag molecular packing model [3] assuming the alkyl chains to be freely rotated about the core axis.

From equations (2) and (3) we note that, without an applied field, the averaged molecular long axis should lie on the *XZ*-plane with $\phi = \pi/2$ [17, 18]. When an electric field is applied, the averaged molecular long axis can rotate from the *XZ*-plane to $\phi = 0$ or π depending on the polarity of the applied voltage. The resulting azimuthal patterns from each IR dipole are presented in figure 5. The table lists the deduced dichroic ratios $D = A_{\parallel}/A_{\perp}$ and the angular shift of azimuthal patterns by the electric field. Note that with a positive applied field the dichroic ratio for IR absorption by atomic segments associated with the FLC core is larger than that with a negative applied field. This suggests that the orientation distributions of these atomic groups are more ordered with a positive voltage than with a negative voltage. For these FLC core groups, the observed angular shifts of the azimuthal patterns are fairly close to the effective cone angle of the FLC medium ($\sim 28^{\circ}$) as shown by equation (2). For CH_2 groups, the dichroic ratios with positive and negative voltages are small and nearly identical. The IR absorption patterns shift only 21°

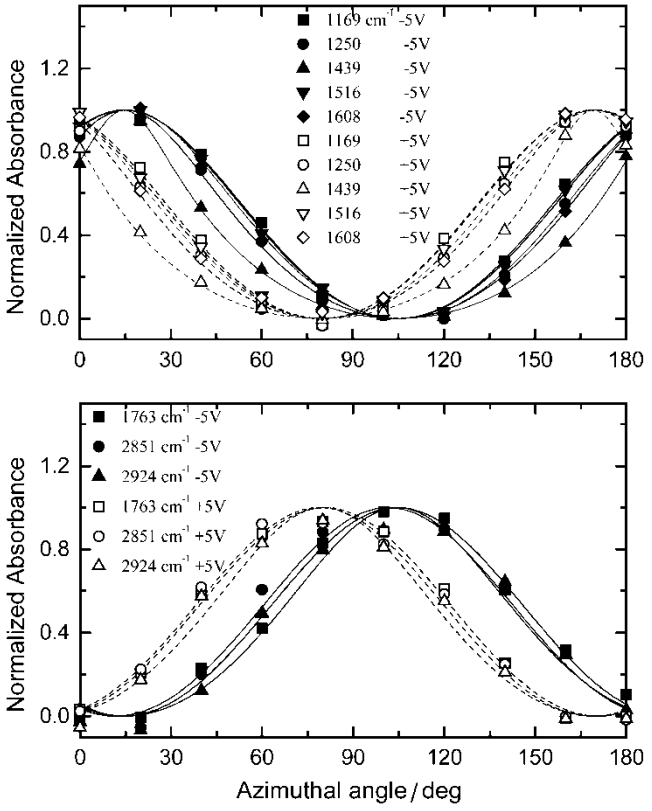

Figure 5. Normalized IR azimuthal patterns of various atomic groups associated with the FLC core (upper), and the alkyl chains and C=O moiety (lower) are presented. Curves with solid symbols are the azimuthal patterns obtained with *negative* voltage while open symbols indicate the result with *positive* voltage.

from +5 to −5 V, reflecting a flexible and less ordered alignment than the core groups. With a given applied voltage, all core group azimuthal patterns form approximately a single pattern, which indicates that none of these atomic groups change their relative orientation in the steady-state alignments with a steady d.c. voltage of opposite polarity. This also appears to be true for CO and CH_2 groups. This is an interesting result considering that each observed IR absorption line can originate from atomic groups which belong to different FLC species, and thus strongly supports that the submolecular fragments in the FLC mixture move in unison with a steady d.c. field.

Table. Dichroic ratio D of infrared absorption peaks and angular shift $\Delta\Phi$ of azimuthal patterns with a steady d.c. field of opposite polarity.

Peak/cm^{-1}	$D(-5\,\mathrm{V})$	$D(+5\,\mathrm{V})$	$\Delta\Phi$/°
1169	5.77	7.30	27
1250	5.39	6.11	26
1439	9.15	9.27	27
1516	7.70	8.08	26
1608	11.30	13.99	27
1763	0.22	0.21	24
2851	0.60	0.57	22
2924	0.39	0.39	21

The model of all FLC species rotating in unison can also be used to describe second harmonic generation. We note that the second harmonic intensity from our SSFLC cell is fairly weak at normal incidence [14]. In order to yield a better SH azimuthal anisotropy we fix the incident angle of the fundamental beam to be about 15°. The resulting SH azimuthal patterns are presented in figure 6 without applying an electric field. The measured SHG patterns qualitatively agree with calculated curves shown in figure 3. The non-vanishing s-in/s-out SH intensity and asymmetric pattern with p-in/s-out suggest that the C_2 symmetry in our SSFLC is partially broken.

As shown in the theoretical analysis, SHG activity from an SSFLC with $\phi = 0°$ or 180° disappears with a maximum SHG signal occurring at $\phi = \pi/2$. By rotating all FLC species in unison from $\phi = 0°$ to 180° with a triangular waveform, we found that the angular position for maximum SHG indeed occurs at $\phi = \pi/2$. The result is shown in figure 7 with a p-in/p-out polarization combination.

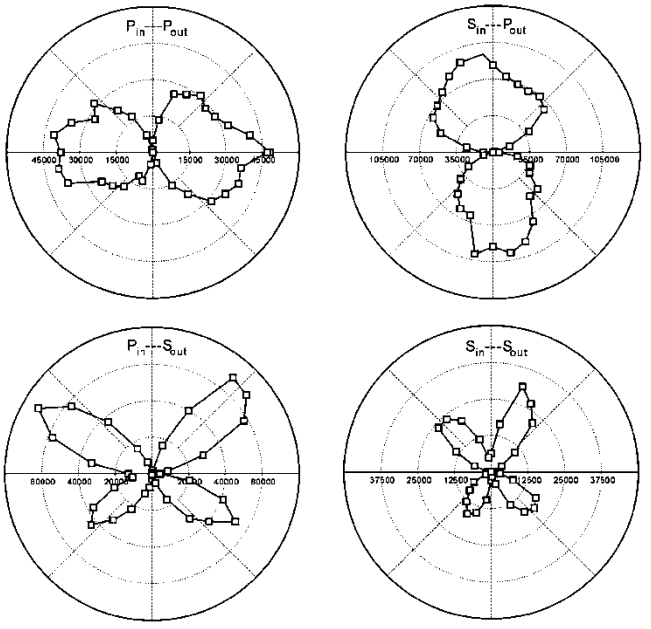

Figure 6. Azimuthal patterns of the second harmonic generation signal from an SSFLC with various polarization combinations. The X-axis (the rubbing direction) of the SSFLC cell is oriented to align with $\Phi = 0$.

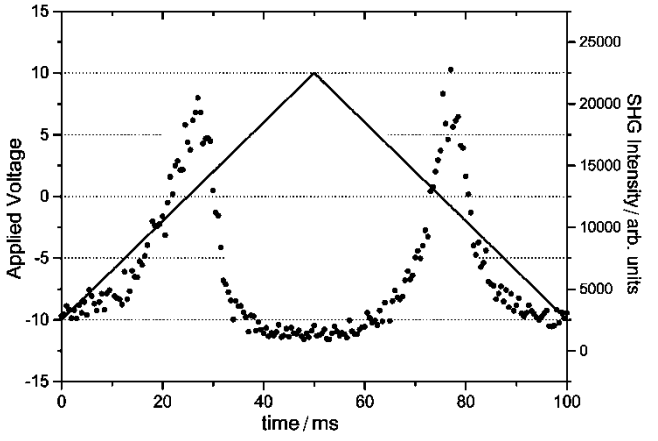

Figure 7. The p-polarized second harmonic signal (filled dots) from an SSFLC cell excited by a p-polarized fundamental beam. The SSFLC cell is driven by a triangular waveform shown by the solid line.

4.2. *Field-induced reorientation*

We now analyse the time-resolved electro-optical response of the SSFLC cell to reveal information about the field-induced reorientation process of the FLC mixture. We insert the SSFLC cell into an optical set-up involving a crossed polarizer-analyser and orient the rubbing direction to align with the transmission axis of the input polarizer. Bipolar square-wave pulses are then employed to excite the SSFLC cell. The field-on period with $+10\,\mathrm{V}$ extends from 0 to 110 μs, followed by a field-free duration ranging from 110 to 500 μs. Then a $-10\,\mathrm{V}$ period extends from 500 to 610 μs. The time-resolved optical transmission is monitored as a function of azimuthal angle of the SSFLC.

From the results presented in figure 8, it can be seen that during the field-on period the symmetry axis of the azimuthal pattern rotates rapidly with a reduction of modulation depth. During the field-free period, the orientation of the azimuthal pattern does not change significantly, instead a slow recovery of the modulation depth is detected. A better presentation can be achieved by fitting the measured patterns to $A(\Phi)=b(t)+a(t)\sin^2[\Phi-\omega(t)]+c(t)\sin^2[2\Phi-2\omega(t)]$. The resulting $a(t)$, $b(t)$, $c(t)$, and $\omega(t)$ are shown in figure 9. The switching time course of the SSFLC director appears to be symmetric in both the positively and negatively driven periods. The contrast ratio of the optical transmission decreases during the field-on period, as shown by a rapid increase of the isotropic component $b(t)$. The isotropic component then slowly decreases with an accompanying increase of $a(t)$ and $c(t)$ after the field is switched off. Note that the optical axis of the SSFLC cell can complete a field-induced rotation in 66 μs, but the molecular segments need a much longer time to adjust to the new optic axis. We believe a detailed

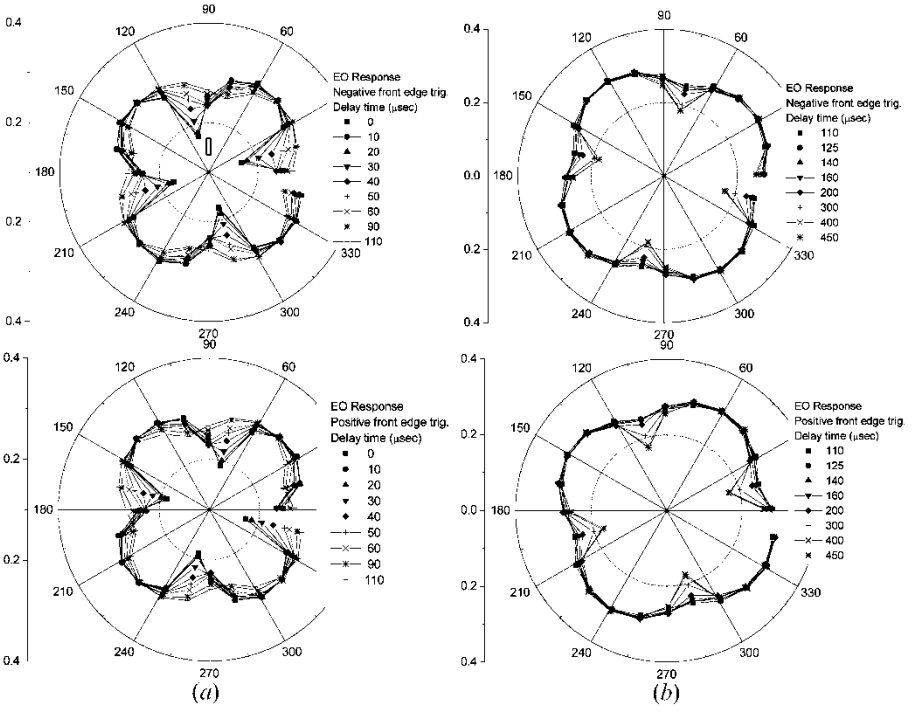

Figure 8. Electro-optical azimuthal patterns measured on an SSFLC during (*a*) the field-on, and (*b*) field-free durations. The direction of the incident polarizer is along the 0 degree. A square-wave voltage pulse of duration 110 μs and amplitude of $-10\,\mathrm{V}$ (top) and $+10\,\mathrm{V}$ (bottom) was used.

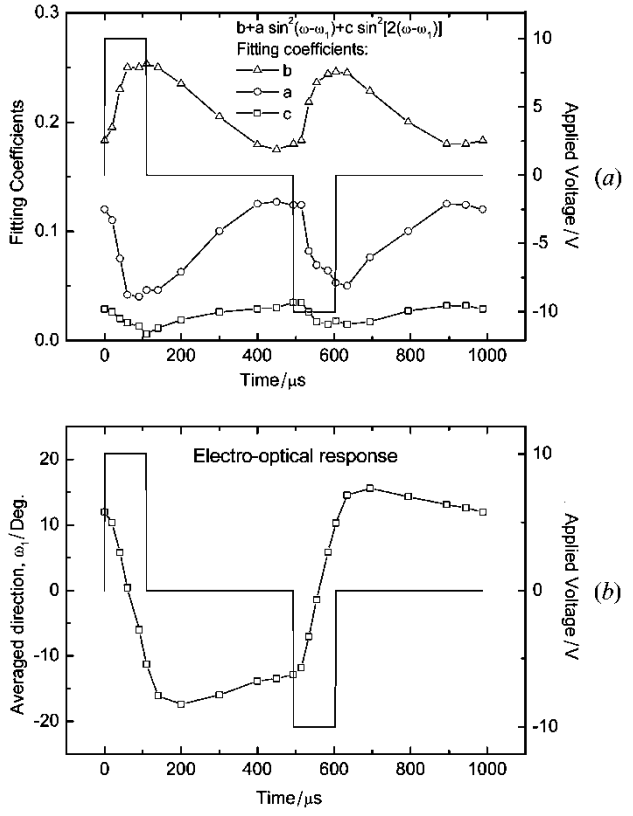

Figure 9. (*a*) Fitting parameters (symbols) of the electro-optical azimuthal patterns and the applied voltage (solid line) are plotted as a function of time. (*b*) The deduced orientation angle of the optic axis of FLC film is shown as open squares. Rubbing direction of the FLC cell is along the 0 degree.

balance among various torques—from ferroelectric, dielectric, elastic and viscous forces—to be responsible for this complex behaviour.

The optical contrast can change with cell thickness, driving voltage and FLC cone angle. In our case, the cell thickness is close to the half-wave thickness of the FLC mixture. The cone angle of our SSFLC (28°) is about 5° away from the desired 22.5°. Therefore the optical contrast of the SSFLC cell is not in the optimum condition. However, based on the dichroic ratio of IR absorption lines listed in the table, we can conclude that the alignment quality of the SSFLC cell is either similar to or even better than results shown in the literature [16]. Furthermore all our SSFLC cells appear single domain under conoscopic examination.

The switching dynamics can be better understood by monitoring the field-induced reorientation of different molecular segments with trFTIR. The results with an SSFLC excited by +10 V from 0 to 110 μs are shown in figure 10.

We note that the orientation distribution of molecular segments with an applied d.c. voltage is narrower than for an SSFLC driven by a pulsed electric field. This reflects the fact that contrast ratio with a d.c. voltage is better than in the dynamic switching process. The FTIR azimuthal patterns of groups of atoms associated with the FLC core reorient, and the resulting angular orientation $\omega(t)$ is shown in figure 11. All the groups of atoms selected are found to follow an almost identical field-on time course of field-induced reorientation. This indicates that the LC cores in the FLC mixture behave somewhat as a rigid unit during the field-on period. However, when the applied field is switched off, all core segments immediately reverse their rotating direction. Then they relax from $\phi \sim 180°$ to the steady-state orientation ($\phi \sim 120°$) with slightly different speeds. This suggests that the core segments in

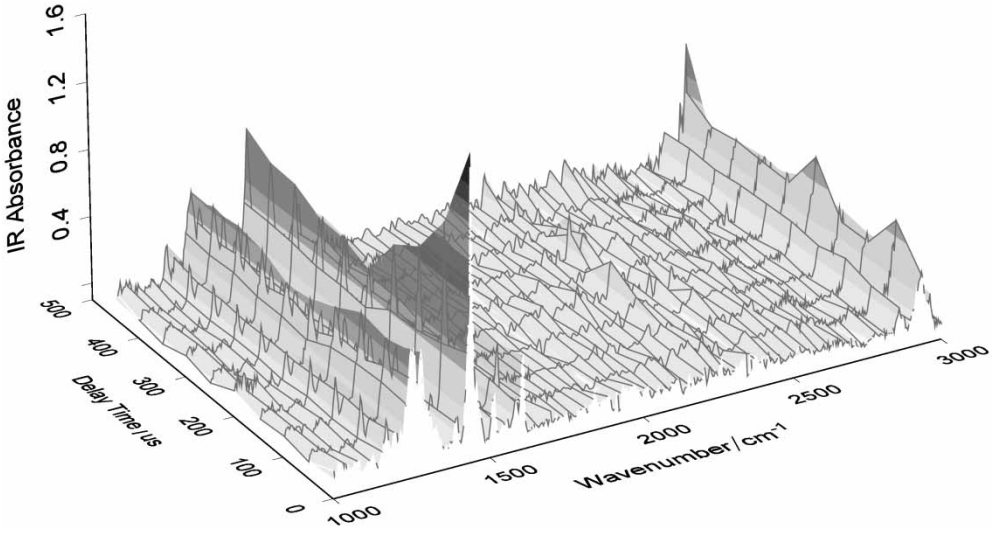

Figure 10. Time-resolved FTIR spectra taken from an SSFLC excited by a +10 V pulse extending from 0 to 110 μs.

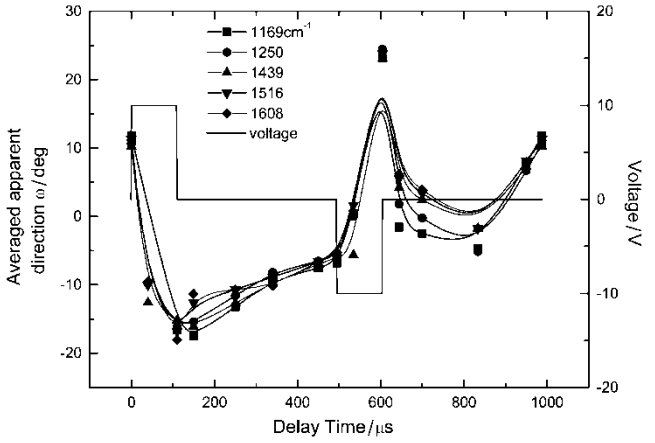

Figure 11. Transient orientations of several molecular segments associated with the FLC cores are presented as a function of delay time. Note that the azimuthal angle can be determined from $\phi(t) = \cos^{-1}[\tan \omega(t)/\tan \theta]$.

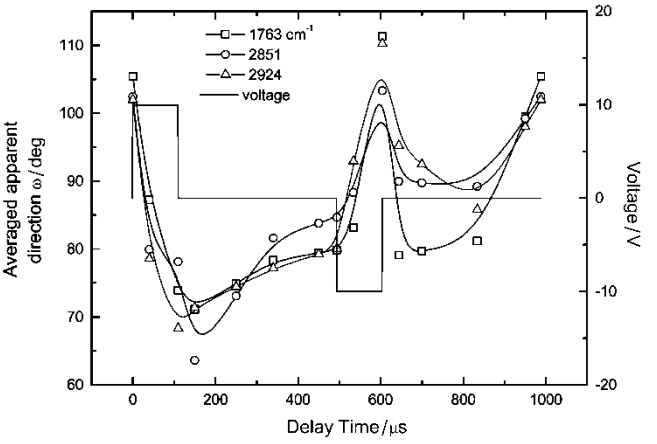

Figure 12. Transient orientations of several molecular segments associated with the C=O moiety and alkyl chain are presented as a function of delay time. The solid lines are a guide for the eye.

the FLC mixture do not behave as a rigid unit in the field-free condition. Apparently, intermolecular interaction among homologous species is not strong enough to forbid different relaxation pathways of the core segments. This behaviour is not seen in the EO measurement. Moreover, unlike the symmetric behaviour in the EO response, our trFTIR study also reveals that the switching process of the core segments in the positively driven period is different from that driven by a negative pulse. The very rapid field-free relaxation observed after the negative driving pulse indicates that the clockwise–anticlockwise symmetry is no longer broken at the molecular level in this FLC mixture. The asymmetry might relate to the mirror symmetry broken in the chiral FLC mixture. Supporting data can also be obtained with SHG, as shown in figure 6, where the p-in/s-out SH azimuthal pattern exhibits asymmetry about the *XZ*-plane and a non-vanishing s-in/s-out SH activity was observed.

For all other groups of atoms not associated with the FLC cores, the time courses of field-induced reorientation are presented in figure 12. As shown in figure 2, the IR polarization with maximum absorbance by these IR dipole moments is perpendicular to the FLC director. Except for the 90° difference, the C=O moiety behaves like the core groups shown in figure 11. For CH_2 on the alkyl chains, a larger deviation from the time course of the core groups was observed, which reflects the more flexible nature of the alkyl chains during the field-induced reorientation process.

5. Summary

We have found from time-resolved electro-optical measurements that all FLC molecules rotate in unison about the layer normal. Although the rotational motion of the FLC director can respond quickly to the applied field, the molecular orientation distribution is found to spread out at first and then slowly converge to the new direction of the FLC director. The azimuthal patterns of FTIR absorption lines associated with the FLC core follow the same time course as shown by the EO measurement with an electric field. When the applied field is switched off, all core segments immediately reverse their rotating direction, and then relax to their steady-state direction with varying relaxation speeds. However, unlike the symmetric behaviour observed with the EO measurement technique, the FTIR time-course reveals that the core segments behave differently in a positive driving field from when driven by a negative pulse. A more rapid field-free relaxation was observed for the core groups after the negative driving pulse. Among groups of atoms not associated with FLC cores, the C=O moiety behaves like those core groups, while CH_2 groups on the alkyl chains are more flexible during the field-induced reorientation process. When the field is switched off, all the core groups relax to the steady-state direction with varying relaxation times. We conclude that submolecular fragments of different molecular species in the FLC mixture can move correlatively in a steady d.c. field and during the field-induced re-orientation process.

We acknowledge financial support from the National Science Council of the Republic of China under grant NSC 91-2112-M-009-037.

References

[1] CLARK, N. A., and LAGERWALL, S. T., 1980, *Appl. Phys. Lett.*, **36,** 899.

[2] LAGERWALL, S. T., 1999, *Ferroelectric and Antiferroelectric Liquid Crystals* (Weinheim: Wiley-VCH).
[3] WALBA, D. M., 1991, Ferroelectric Liquid Crystals: A Unique State of Matter, in *Advances in the Synthesis and Reactivity of Solids*, vol. 1 (JAI Press Ltd.), pp.173–235.
[4] PARK, B., NAKATA, M., SEOMUN, S., TAKANISHI, Y., ISHIKAWA, K., and TAKEZOE, H., 1999, *Phys. Rev. E*, **59,** R3815.
[5] JANG, W. G., PARK, C. S., and CLARK, N. A., 2000, *Phys. Rev. E*, **62,** 5154.
[6] ZHAO, J. G., YOSHIHARA, T., SIESLER, H. W., and OZAKI, Y., 2002, *Phy. Rev. E*, **65,** 0 217 104.
[7] HIDE, F., CLARK, N. A., NITO, K., YASUDA, A., and WALBA, D. M., 1995, *Phys. Rev. Lett.*, **75,** 2344.
[8] SHILOV, S. V., SKUPIN, H., KREMER, F., WITTIG, T., and ZENTEL, R., 1997, *Phys. Rev. Lett.*, **79,** 1668.
[9] VERMA, A. L., ZHAO, B., TERAUCHI, H., and OZAKI, Y., 1999, *Phys. Rev. E*, **59,** 1868.
[10] KOCOT, A., WZRALIK, R., ORGASINGKA, B., PEROVA, T., VIJ, J. K., and NGUYEN, H. T., 1999, *Phys. Rev. E*, **59,** 551.
[11] MASUTANI, K., SUGISAWA, H., YOKOTA, A., FURUKAWA, Y., and TASUMI, M., 1992, *Appl. Spectrosc.*, **46,** 560.
[12] SKUPIN, H., KREMER, F., SHILOV, S. V., STEIN, P., and FINKELMANN, H., 1999, *Macromolecules*, **32,** 3746.
[13] SHEN, Y. R. *The Principles of Nonlinear Optics* (New York: John Wiley), pp. 67–87.
[14] FOKIN, Y. G., MURZINA, T. V., AKTSIPETROV, O. A., SORIA, S., and MAROWSKY, G., 2002, *Appl. Phys. B*, **74,** 777.
[15] ZHAO, J. G., YOSHIHARA, T., SIESLER, H. W., and OZAKI, Y., 2001, *Phys. Rev. E*, **64,** 031 704.
[16] VERMA, A. L., ZHAO, B., BHATTACHARJEE, A., and OZAKI, Y., 2001, *Phys. Rev. E*, **63,** 051 704.
[17] BROWN, C. V., and JONES, J. C., 1999, *Appl. Phys. Lett.*, **86,** 3333.
[18] VAUPOTIC, N., GRUBELNIK, V., and COPIC, M., 2000, *Phys. Rev. E*, **62,** 2317.